THE JOURNAL OF PHYSICAL CHEMISTRY C

pubs.acs.org/JPCC

Article

Studying Chemisorption at Metal−Polymer Interfaces by Complementary Use of Attenuated Total Reflection−Fourier Transform Infrared Spectroscopy (ATR-FTIR) in the Kretschmann Geometry and Visible−Infrared Sum-Frequency Generation Spectroscopy (SFG)

Laura-Lynn I. Fockaert, Deborah Ganzinga-Jurg, Jan Versluis, Berend Boelen, Huib J. Bakker, Herman Terryn, and Johannes M. C. Mol*

Cite This: J. Phys. Chem. C 2020, 124, 7127−7138

Read Online

ACCESS | Metrics & More | Article Recommendations

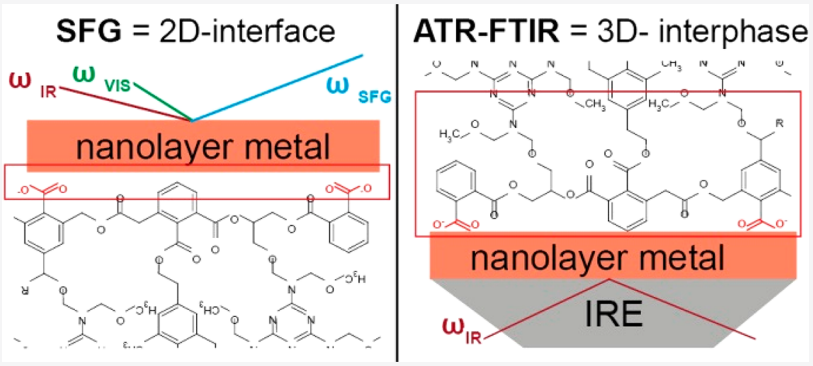

ABSTRACT: The molecular configuration and chemistry at the zinc/zinc oxide−polyester interface were studied by using two complementary spectroscopic techniques: attenuated total reflection−Fourier transform infrared spectroscopy (ATR-FTIR) and sum-frequency generation (SFG) spectroscopy. It was shown that ATR-FTIR should be considered as a (3D) interphase-sensitive technique with probing depths of 250−400 nm in the headgroup region (2000−1200 cm^{-1}). On the other hand, SFG is known to be a (2D) interface-sensitive technique. The ATR-FTIR measurements showed that carboxylate groups are formed within the near-interface region of the polyester phase. SFG measurements showed that the carboxylic acid groups are stable at the polymer−zinc/zinc oxide interface. In addition, in situ ATR-FTIR and SFG measurements have been conducted when exposing the polyester−zinc/zinc oxide system to D_2O. The exposure to D_2O is observed to lead to an additional conversion of ester and carboxylic acid groups to carboxylate groups. The comparison of the SFG and ATR-FTIR measurements shows that this conversion occurs much slower at the polyester−zinc/zinc oxide interface than in the bulk of the polyester. Finally, the strengths and limitations as well as the complementarity of both techniques are discussed.

1. INTRODUCTION

Polymer−metal (oxide) hybrid systems are widely used in numerous applications, among others as protective coatings against corrosion of underlying metals.[1−4] For this purpose, a highly stable polymer−metal (oxide) interface is desired to preserve the substrate during its service life. Consequently, a detailed understanding of the interface between polymer and metal (oxide) is crucial for a systematic design of durable polymer−metal (oxide) hybrid systems. A challenge in this regard is to access this buried interface and to obtain representative information regarding the interfacial molecular structure. For this purpose, specific analytical tools are required which are sufficiently surface sensitive, on the one hand, and can access the buried interface, on the other.[5] Conventional surface sensitive tools, however, often fail to access the buried interface.[6,7] A nondestructive approach in studying the buried polymer−metal (oxide) interface is the application of thin films either as the polymer coating, where solvent evaporation is

Received: November 18, 2019
Revised: March 7, 2020
Published: March 9, 2020

used to apply nanolayers of model polymer coatings on metal oxides,[8−11] or as a thin metal (oxide) layer in contact with polymer coating, which provides access to the buried interface from the metal (oxide) side.[12−15] The majority of vibrational studies, i.e., infrared reflection−absorption spectroscopy (IRRAS),[16−20] attenuated total reflection−Fourier transform infrared spectroscopy (ATR-FTIR),[10,11,21−26] and visible infrared sum frequency generation (SFG)[27−32] on metal−polymer interfaces, have been conducted by using thin organic films approaching the buried interface nondestructively from the polymer side.

An additional advantage of the thin film approach is the simplified organic film chemistry which facilitates spectral interpretations. Chemisorption of model molecules as thin adsorbate layers has proven to be a useful methodology to mimic polymer adhesion on solid substrates and has resulted in new fundamental insights into chemisorption mechanisms.[11,24,33−36] Using infrared spectroscopy, we have probed interfacial metal−molecule bonds for carboxylic acids and ester-functionalized compounds, resulting in the formation of metal−carboxylate complexes.[11,22,23,37−39] Moreover, amine- and amide-functionalized compounds were shown to interact through Lewis acid−base interactions with their electron-rich nitrogen and oxygen atoms.[24,40] These common functional groups which are held responsible for bonding have their major absorption bands in the IR region ranging from 1900 to 1300 cm^{-1}. However, because of experimental limitations, existing literature on metal−polymer interfaces studied by means of SFG mainly focuses on the O−H and C−H stretch region, i.e., 3800−2400 cm^{-1}.[41,42] Yet, the share of SFG studies on the functional headgroup region, i.e., 1900−1300 cm^{-1}, is growing due to recent advantages in laser technology. Adhikari et al. performed SFG studies on solid−liquid interfaces studying the interaction of methacrylate-based monomers at the hydrophilic quartz surface. This elucidated the presence of carbonyl peak near the quartz surface, which was not observed at the air interface. From this, it was inferred that methacrylate carbonyl bonds were involved in hydrogen bonding with the Si−OH groups of the quartz, inducing increased orientation at the quartz interface, which was not established at the air interface.[31] Furthermore, the tilt angle of oriented carbonyl bonds can be experimentally determined by performing a comparative study of the carbonyl SF intensity obtained using SSP, SPS, and PPP polarization modes.[32] Tang et al. studied deprotonation mechanisms of carboxylic acids groups and induced by various metal cations, i.e., K^+, Na^+,[43] Ca^{2+}, and Mg^{2+},[44] indicating varying ionic strength of the metal−carboxylate complexes associated with the interacting metal cation.

Now, these fundamental insights need to be translated to industrially relevant polymer coating systems. Polyester resins are widely applied in flexible and rigid packaging, automotive paints, can and coil coating, and industrial paints. However, since paint formulations are composed of multiple components, such as curing agents, cross-linkers, corrosion-inhibiting pigments, adhesion promotors, and so on, their adhesion properties do not solely result from resin chemistry.[45−47] Moreover, polyester paints are typically applied in the micrometer range and require a curing step, which is known to induce conformational changes and to alter bond formation kinetics and strengths.[45,48] This requires the use of the thin substrate approach since industrial paints are generally applied in the micrometer scale.

Presumably the most accessible and user-friendly spectroscopic tool to do so is ATR-FTIR in the Kretschmann geometry.[12−14] In the Kretschmann geometry, a nanolayered metal (oxide) film, transparent for the IR beam, is brought in direct contact with an internal reflection element (IRE). Upon reflection from the internal surface of the IRE, an evanescent wave is created and projected orthogonally into the sample. The depth of this evanescent wave passing the nanolayered metal film into the polymer coating is a subject of ongoing debate.[49] It is known that some transition metals are capable of inducing an enhancement effect in the Kretschmann configuration, also known as surface-enhanced infrared adsorption (SEIRA).[50,51] Because of this enhancement, vibrational modes in the first monolayer (within 5 nm) directly attached to the surface show a 10−1000 times more intense absorption compared to measurements without metal.[50,51] Two mechanisms have been proposed to contribute to the total enhancement; the electromagnetic (EM) and chemical mechanism (CM). The first mechanism only occurs on discontinuous films, typically thinner than 10 nm.[50] The second mechanism relates to chemical effects, such as charge-transfer interactions between the adsorbate and the metal. Vibrational modes involving modulations of the dipole moment perpendicular to the metal surface are preferentially enhanced.[51] Some transition metals are capable of inducing such an enhancement effect, but these have rarely been studied. This is because the enhancement is more significant for noble metals and therefore unlikely to occur for metals relevant for metal (oxide)−polymer hybrid systems.[51] Consequently ATR-FTIR with reported probing depths from 100 nm to several micrometers should not be considered as a surface-sensitive technique.[52,53] Nevertheless, ATR-FTIR spectra are frequently considered to represent metal−polymer interfacial information.[12−15,48,54]

SFG, on the other hand, is a second-order nonlinear technique providing truly interface-sensitive and selective molecular information due to the fact that it requires symmetry breaking.[41,55] Strongly polar oriented interfaces therefore generate an SFG signal where the symmetry is broken and which explains the absence of SFG signal in centrosymmetric media, which is the case for most bulk materials.[56] To generate a SFG signal, molecular bonds thus need to be highly oriented at the interface, thereby creating a broken inversion symmetry at the interface. Moreover, the molecular bonds need to be both IR- and Raman-active, and the two incident light beams (narrow-band VIS and broad-band IR) need to overlap in both space and time at the unknown interface. Because of these strict selection rules, SFG spectra are in general less complex and inherently surface sensitive—two major advantages compared to ATR-FTIR Kretschmann when studying industrially relevant multicomponent paints. However, up to now, such SFG measurements have not been conducted before. Overall, very few studies on the application of SFG to metal−polymer interfaces have been reported.[57] Most likely this is due to the complexity of the SFG setup and experimental limitations in using SFG in the mid-IR region. Because of these experimental limitations, the existing literature mainly focuses on the O−H and C−H stretch region, i.e., 3800−2400 cm^{-1}.[41,42] In addition, the SFG signal from the metal−polymer interface needs to be distinguished from that of the polymer−air interface.[55,58−60] Recent developments in laser technology opened up the mid-IR region up to 1200 cm^{-1} for SFG studies,[61,62] giving access to

https://dx.doi.org/10.1021/acs.jpcc.9b10775
J. Phys. Chem. C 2020, 124, 7127−7138

Table 1. Polyester Clear Coat Formulation

compound	quantity (wt %)	function	chemistry + properties
Dynapol LH 820-16/55%	70.2	polyester resin	saturated, medium molecular (MM 5000 g/mol), linear hydroxylated copolyester resin. TG = 60 °C (acid value of 2 mg KOH/g and an OH value of 20 mg KOH/g)
Cymel 303	5.5	cross-linker	highly methylated monomeric melamine-based cross-linker (methoxy methyl functional sites)
Dynapol Catalyst 1203	2.1	catalyst for cross-linker	nonionic blocked sulfonic acid catalyst for aminoplast cross-linking
Solvent Naphtha 200	11.0	solvent	aromatic solvent
butyl diglycol	4.6	solvent	$HO-(CH_2)_2-O-(CH_2)_2-(CH_2)_3CH_3$
butyl glycol	6.6	solvent	$CH_3-(CH_2)_3-O-CH_2-OH$

the vibrational modes of carboxylic groups such as carbonyl (C═O) stretch vibrations and carboxylate (COO^-) stretch vibrations. As a result, SFG can become a valuable analytical tool in a broad range of research fields.

Up to now, SFG studies of buried polymer−metal interfaces have been limited to model polymer systems on the nanoscale. Hence, an appropriate experimental approach needs to be developed that allows the investigation of realistic paint films in the micrometer range with SFG.

This work describes the chemical bond formation of an industrially relevant polyester coil coat and zinc/zinc oxide substrate. We perform a comparative study with ATR-FTIR and SFG to reveal to what extent the chemical information obtained from ATR-FTIR spectra measured in a Kretschmann configuration represents the interfacial properties of polyester-coated zinc oxide. Moreover, an experimental configuration suitable for in situ SFG measurements has been developed to probe interfacial bond degradation during exposure to an aqueous environment. Finally, the strengths and limitations of both spectroscopic techniques are being compared to illustrate the complementarity of the two vibrational techniques.

2. EXPERIMENTAL SECTION

2.1. ATR-FTIR in Kretschmann Configuration. The FTIR apparatus was a Thermo-Nicolet Nexus equipped with a liquid-nitrogen-cooled mercury−cadmium−telluride (MCT-A) detector and a nitrogen-purged measurement chamber with a Veemax III single reflection ATR accessory. Germanium IRE (PIKE Technologies) with a fixed face angle of 60° were used. IR light was configured with an incident set angle of 80°. A precision manual polarizer (PIKE) was mounted on the Veemax III and set to 90° for p-polarized and 0° for s-polarized IR light. For the chemisorption studies infrared backgrounds were obtained from the metallic coated IRE. The established interfacial chemistry was followed in situ in aqueous environment by using D_2O (99.9%, Sigma-Aldrich). D_2O was chosen instead of H_2O because of the shift of the bending vibrations toward lower wavenumbers (1200 cm^{-1} for O−D vs 1640 cm^{-1} for O−H). This shift allows us to probe the asymmetric carboxylate stretching vibrations established at the zinc oxide surface. For these in situ stability studies, infrared backgrounds were obtained after applying the polymer coating on the respective metal oxides. Consequently, as the interfacial chemistry established after curing was involved in the background, the evolution of interfacial bonds may appear positive when being increased or negative when being reduced relative to the initial dry (cured) situation. Infrared spectra were collected every 300 s and averaged from 128 cycles with a resolution of 4 cm^{-1}. The control of the spectra acquisition and incident angles was managed by the OMNIC 8.1 software package (ThermoElectron Corporation, Madison, WI).

2.2. ATR-FTIR Samples. 50 nm zinc (Goodfellow, 99.95%) was deposited on germanium internal reflection elements (IRE) by means of a high-vacuum evaporation system (VCM 600 Standard Vacuum Thermal Evaporator, Norm Electronics). A polymer coating with polyester-based resin, Dynapol LH 820 (Evonik Industries AG), was applied by using a 30 μm bar coater. The resulting polymer film was cured for 15 min at 130 °C, which is the maximum operating temperature for germanium IRE. The polyester primer formulation can be found in Table 1.

2.3. Surface Sum-Frequency Generation (SFG) Spectroscopy. The laser source used is a Ti:sapphire laser system which consist of an oscillator (Coherent Mantis) and an amplifier (Coherent Legend Duo) generating 35 fs pulses of a broadband beam with a wavelength of 795 nm, a 6.5 mJ pulse energy, and a repetition rate of 1 kHz. The VIS pulse is prepared by transmitting ∼20% of the amplifier output through an pulse shaper/monochromator to reduce its spectral bandwidth, yielding a 15 μJ pulse with a FWHM of 15 cm^{-1}. The remaining amplifier output passes through an optical parametric amplification (OPA) process (Light Conversion HE-TOPAS) to generate mid-IR broad-band pulses tunable in the range 1200−4000 cm^{-1} with a FWHM of ∼400 cm^{-1}.[63] The mid-IR broad-band pulse is subsequently sent through a long-wave pass filter to filter out the signal and idler beams. The VIS beam is guided through a delay stage to adjust the travel time to that of the IR beam in the OPA. Thereby temporal overlap of the beams is achieved which is a prerequisite for SFG. The intensity of the beams was controlled with a half-wave plate and a polarizer in the beam paths and by adjusting the apertures of the IR and VIS beams. Final intensities were 10 mW for the IR beam and 3.8 mW for the VIS beam which were focused on the sample to generate SFG upon spatial and temporal overlap. The reflected SFG beam passes two notch filters to filter out the residual VIS light and a polarizer to select the SFG polarization. Finally, an SFG signal obtained with an SSP polarization configuration (SFG = s-polarized, vis = s-polarized, IR = p-polarized) is focused on the detector slit (PIXIS 100B camera with an SP-2-300i spectrograph). For measurements in the frequency region of the carbonyl and carboxylate stretch vibrations (1300−1900 cm^{-1}) the setup was purged with nitrogen to avoid environmental interference. SFG measurements in the 3000−2400 cm^{-1} region were performed without nitrogen flushing. Because of the low damage threshold of the samples, integration times were limited to a maximum of 300 s. To normalize the SFG signal and to monitor the stability of the laser, an SFG spectrum of a quartz plate was taken regularly,

https://dx.doi.org/10.1021/acs.jpcc.9b10775
J. Phys. Chem. C 2020, 124, 7127−7138

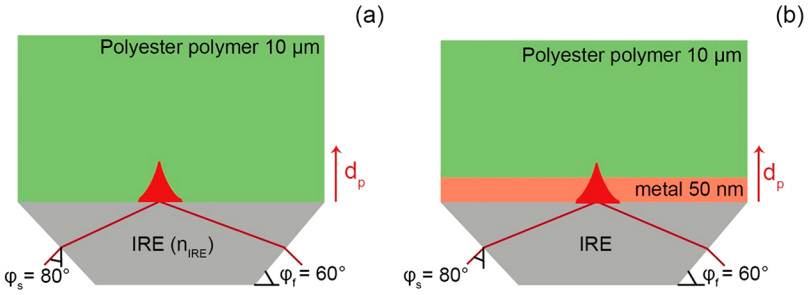

Figure 1. (a) Polyester-coated IRE (two-layered system) and (b) polyester-coated zinc deposited on internal reflection element (three-layered system).

with an integration time of 10 s. The measured SFG spectra were corrected for the background and normalized with a corresponding spectrum of quartz.

2.4. SFG Samples. The 6 nm zinc films were sputtered on CaF_2 windows (ϕ 25 mm, thickness 2 mm, Crystal-GmbH) by means of a LEICA SCD 500 sputter coater using a zinc target (99.9%, Chempur GmbH) at a argon pressure of 10^{-2} mbar. Prior to the zinc film application, the CaF_2 windows were cleaned by means of argon sputtering. A polyester clear coat was applied on both clear CaF_2 and zinc-coated CaF_2 windows by spin-coating using a rotation speed of 2500 rpm for 1 min, resulting in a final coating thickness of 10 μm.

3. RESULTS AND DISCUSSION

3.1. Attenuated Total Reflection–Fourier Transform Infrared Spectroscopy (ATR-FTIR). ATR-FTIR was performed on two-layered (Ge–polyester coating) and three-layered (Ge–zinc/zinc oxide–polyester coating) systems whose configurations are illustrated in Figure 1.

From Harrick's equations[49,52] (eqs 1–4) it can be seen that the depth of penetration (d_p) varies with the incident IR angle (φ_{eff}), frequency of the IR beam (λ), and the refractive indexes of the germanium reflection element ($n_{IRE} = 4$), zinc (n_{Zn}), and polyester coating ($n_{PE} = 1.5$). The effective incident IR angle (φ_{eff}) results from eq 3, which takes into account the face angle of the germanium IRE (φ_f), fixed at 60°, and the set angle for the incident IR beam (φ_s) set at 80° as illustrated in Figure 1.

$$d_{p-2} = \frac{\lambda}{2\pi(n_{IRE}^2 \sin^2 \varphi_{eff} - n_{PE}^2)^{1/2}} \quad (1)$$

$$d_{p-3} = \frac{\lambda}{2\pi n_m \left(\sin^2 \varphi_2 - \left(\frac{n_{PE}}{n_{Zn}}\right)^2\right)^{1/2}} \quad (2)$$

$$\varphi_{eff} = \varphi_f + \sin^{-1}\left(\frac{\sin(\varphi_s - \varphi_f)}{n_{IRE}}\right) \quad (3)$$

$$\varphi_2 = \sin^{-1}\left(\sin \varphi_{eff} \frac{n_{IRE}}{n_{Zn(\lambda)}}\right) \quad (4)$$

The refractive index of the polyester coating and germanium IRE are considered to be constant over the studied IR frequency range, being 1.5 and 4, respectively. Conversely, metals are characterized by a complex refractive index N, expressed as $N = n + i\kappa$, with n, being the magnitude of the refractive index, which is equal to the ratio of phase velocity of light in a vacuum to those in medium. The imaginary part of the refractive index corresponds to the extinction coefficient κ, which expresses the exponential decay of the electromagnetic wave when propagating through a medium.[64] Both values highly depend on the IR frequency, as shown by the values reported by Querry et al.,[65] given in Table 2. However, the

Table 2. Real and Imaginary Parts of the Complex Refractive Index of Zinc According to Querry et al.[65]

ν/cm^{-1}	$\lambda/\mu m$	n_{Zn}	κ_{Zn}
4000	2.50	6.3	26.5
1700	5.88	21.4	57.7
600	16.67	58.1	100.9

depth of penetration in metals (termed skin depth) depends rather weakly on the wavelength, while that in dielectrics increases fast and nonlinearly with the wavelength (typically on the order of $\lambda/2$).[66] The depth of penetration into the metal (skin depth) gives a measure on the coupling strength between the evanescent wave induced during internal reflection and the propagating surface plasmons polariton and is directly related to the extinction coefficient. Meanwhile, the depth of penetration is majorly determined by the real part of the refraction index.[49] Strictly speaking, one should differentiate between zinc and zinc oxide, considering a four-layered system instead of three-layered system. However, the refractive index of monoclinic zinc oxide is close to that of the polyester coating (i.e., 1.5). Therefore, because of the experimental difficulties on obtaining reliable refractive index values for metal oxides as well as the their close approximation to the refractive index of polyester, the contribution of the zinc oxide layer to the estimated depth of penetration is assumed to be negligible.

The estimated values for the depth of penetration for a two- and three-layered system (d_{p-2} and d_{p-3}) are illustrated in Figure 2. It can be seen that the Harrick's equations give similar outcomes for a configuration with and without metallic film (three- and two-layered system, respectively). On the other hand, the IR wavenumber is shown to play a predominant role in the depth of penetration. The maximum incident set angle of 80°, considered as most interfacial sensitive, results in an estimated depth of penetration of 250–400 nm in the IR frequency region of interest, which is the headgroup region between 1200 and 2000 cm^{-1}.

Based on Harrick's equations, the probing depth of ATR-FTIR is thus considered to be equal with and without a metallic film. However, the sensitivity of ATR-FTIR can be limited to the first monolayer when the metallic film introduces a surface enhancement effect.

https://dx.doi.org/10.1021/acs.jpcc.9b10775
J. Phys. Chem. C 2020, 124, 7127–7138

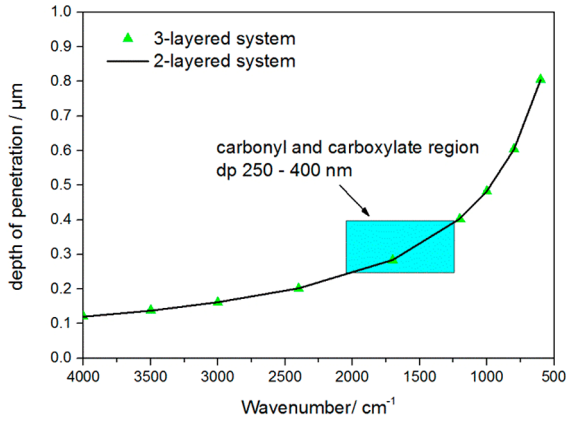

Figure 2. Depth of penetration calculated according to Harrick's equations.

Figure 3 presents ATR-FTIR spectra for a two- and three-layered system collected with p- and s-polarized IR light.

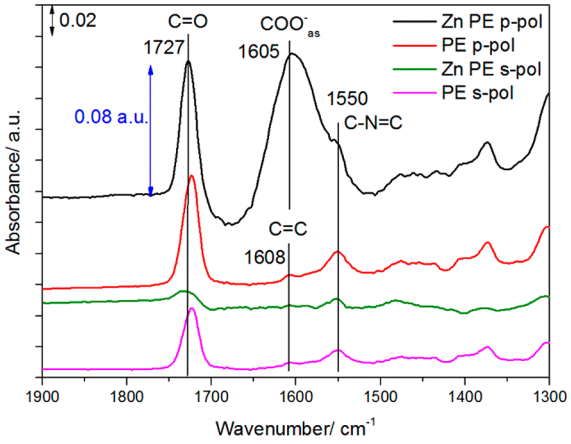

Figure 3. ATR-FTIR spectra of polymer-coated zinc on germanium IRE obtained by using s- and p-polarized IR light and ATR-FTIR spectra of polymer-coated germanium IRE obtained by using s- and p-polarized IR light.

Because the ATR-FTIR spectra are expressed in a common scale, the magnitudes of the spectral peaks in absence and presence of a metallic film can be compared. The presence of the metallic layer does not lead to a significant enhancement of the absorption. Hence, there appears to be no chemical enhancement effect due to chemisorption of functional groups at the zinc oxide surface and also no electromagnetic enhancement effect. The latter can be explained from the relatively large film thickness (50 nm), resulting in a continuous zinc film. Consequently, since no enhancement effects are shown to occur, ATR-FTIR interface studies on zinc–polyester hybrid systems cover an interface region 250–400 nm in the headgroup region, as illustrated in Figure 2. This means that the ATR-FTIR measurements should be considered as an interphase-sensitive tool rather than an interface-sensitive tool. Whereas interfaces are characterized by their two-dimensional properties, interphases have a significant additional dimension in depth.

The p-polarized ATR-FTIR spectrum of the sample with zinc shows a strong additional spectral feature positioned at 1605 cm^{-1} in comparison to the p-polarized ATR-FTIR spectrum of the sample without zinc (Figure 3). This additional peak can be assigned to the asymmetric carboxylate stretch vibrations and signals the establishment of interfacial carboxylate bonds at the zinc oxide–polyester interface.[11] That this peak is much more intense when using p-polarized IR light and practically absent when using s-polarized IR light indicates that the transition dipole moment of asymmetric stretch vibrations occurs highly perpendicular to the surface. In our previous work, we attributed this to a monodentate zinc–carboxylate coordination.[67]

3.2. Sum Frequency Generation Spectroscopy (SFG).

3.2.1. Measurement Schemes for SFG Measurements. The majority of SFG studies on metal–polymer interfaces are conducted in a top configuration,[41,55,60,68] meaning that the laser beams reach the interface from the polymer side, as illustrated in Figure 4A,B.

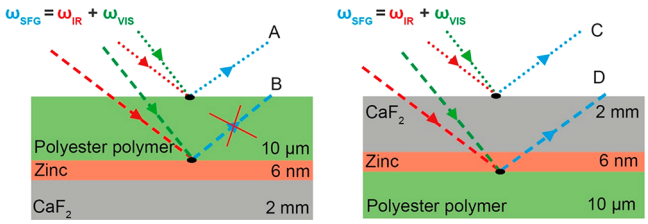

Figure 4. Laser beam configuration used to study metal–polymer interfaces: (A) top configuration, polyester–air interface; (B) top configuration, polyester–zinc/zinc oxide interface; (C) inverse configuration, CaF_2–air interface; (D) inverse configuration, zinc/zinc oxide–polyester interface.

This top configuration is a useful layout when the photons of the incident beams are hardly adsorbed by the polymer layer, which assumption is met in case the polymer film is sufficiently thin, i.e., nanometer scale.[41] For such thin polymer films the interfaces A and B are measured simultaneously, and thus additional efforts have to be taken to separate the SFG signals from the respective interfaces.[41,55,69] In this work polyester coatings with a thickness of 10 μm are being studied; the transmission FTIR spectrum is shown in Figure 5. The molecular bonds given in blue are associated with components present in the polyester resin, whereas the green ring structure positioned at 1552 cm^{-1} is assigned to the melamine rings originating from the cross-linker. The saturated peaks positioned at 1728 and 1244 cm^{-1}, shown in red, evidence

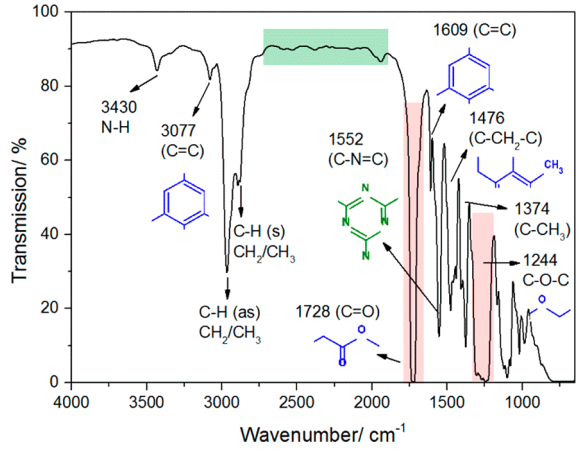

Figure 5. Transmission FTIR spectrum of 10 μm polyester coating.

https://dx.doi.org/10.1021/acs.jpcc.9b10775
J. Phys. Chem. C 2020, 124, 7127–7138

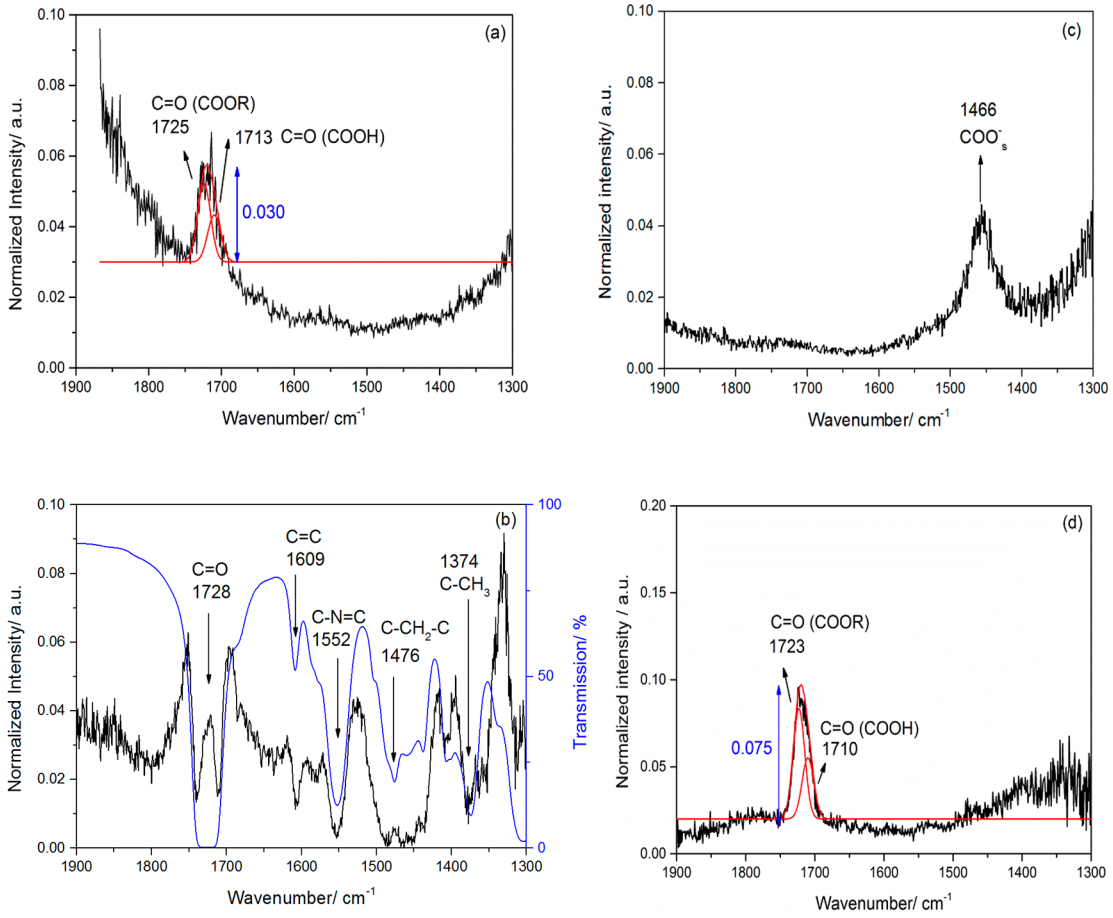

Figure 6. (a) SFG spectrum of the polyester–air interface collected by using the top configuration. (b) SFG spectrum of the polyester–zinc interface collected by using top configuration, with transmission FTIR spectrum shown in blue on the secondary *y*-axes. (c) SFG spectrum of the CaF_2–air interface obtained in inverse configuration. (d) SFG spectrum of the zinc–polyester interface obtained in inverse configuration. The ester and acid carbonyl subpeaks have been fitted by using a FWHM of 18 cm^{-1}.

that highly polar C═O and C–O bonds fully absorb incident IR light. Conversely, no or limited IR absorption is shown to take place in the IR frequency region ranging from 2000 to 2700 cm^{-1}, indicated in green. This because of the absence of molecular bonds that vibrate in this specific region. Consequently, the top configuration is not ideal for studying buried metal–paint interfaces in the IR frequency region of interest. An alternative is the inverse configuration demonstrated in Figure 4C,D. In this configuration the metal–polymer interface is reached from the metal side. This requires the metal film to be sufficiently thin to be transparent for both IR and visible light.

In Figure 6a,b we present SFG spectra measured for CaF_2–polyester and CaF_2–zinc/zinc oxide–polyester samples in top configuration. The SFG spectrum shown in Figure 6a is dominated by the response of the polyester–air interface (interface A). Only one peak positioned at 1720 cm^{-1} appears in the carbonyl/carboxylate region (1900–1300 cm^{-1}) that can be assigned to carbonyl (C═O) stretching vibrations. A comparison of this SFG spectrum with the ATR-FTIR spectrum of polyester in the absence of zinc/zinc oxide, shown in Figure 3, shows that remarkably fewer vibrations are SFG-active than IR-active. The SFG spectrum of the CaF_2–zinc/zinc oxide–polyester sample in the top configuration, shown in Figure 6b, is much more complex. Such significant variations between SFG spectra obtained at interfaces A and B are unexpected since it concerns the same polymer layer with a similar chemical composition. The only chemical difference that is expected to occur between both interfaces is the establishment of interfacial carboxylate bonds at the zinc–polyester interface as shown by ATR-FTIR in Figure 3. Furthermore, it is noted that the spectrum shown in Figure 6b coexists of positive and negative peak intensities. The occurrence of dips in the spectrum is associated with a combination of the broad nonresonant SFG response of the zinc oxide and IR absorption effects of the polyester layer absorption of IR light by the 10 μm thick polyester coating. The presence of positive peaks implies that the nonresonant signal of zinc oxide is not very strong. Nonetheless, the complex response of interface B confirms that the top configuration is not a suitable approach for studying buried interfaces covered with macro-coatings.

The SFG spectra of CaF_2–polyester and CaF_2–zinc/zinc oxide–polyester samples measured in the inverse configuration are shown in Figure 6c,d. In this configuration the response of the CaF_2–air interface C can be spatially distinguished from that of the zinc/zinc oxide–polyester interface D, thanks to the fact that the CaF_2 has a thickness of 2 mm.

The spectrum of interface C, given in Figure 6c, shows a single peak at 1466 cm^{-1} that can be assigned to symmetric carboxylate (COO^-_s) stretching vibrations.[70] This band shows the adsorption of carboxylate species to the CaF_2 surface and

https://dx.doi.org/10.1021/acs.jpcc.9b10775
J. Phys. Chem. C 2020, 124, 7127–7138

originates from ambient carbon contaminants. The presence of this band illustrates that CaF_2 is not as chemically inert as germanium. The SFG spectrum shown in Figure 6d represents the spectrum of the zinc/zinc oxide−polymer interface, and it is interesting to compare this spectrum with of the nonreacted polyester of Figure 6a. It is seen that the carbonyl peaks consist of two contributions, i.e., a major peak at 1723 cm^{-1} representative for carbonyl bonds specific to ester groups and a shoulder at 1710 cm^{-1} attributed to carbonyl bonds of acid groups.[71] The increased carbonyl peak intensity in the presence of zinc (0.075 au) vs nonreacted polyester (0.030 au) refers to an increased fraction of strongly oriented ester and acid carbonyl groups near the zinc and zinc oxide. Interestingly, the SFG spectrum only shows the presence of acid groups (COOH) and not of deprotonated carboxylate (COO^-) at the zinc oxide interface. One possible explanation for this difference is that the SFG spectrum only represents the response of the carboxylic acid groups in molecular proximity of the zinc and zinc oxide surface, whereas the ATR-FTIR spectrum represents the properties of the full bulk-like polyester phase. It could be that the nearby presence of zinc and zinc oxide stabilizes the COOH groups. In addition, the physicochemical properties of the zinc/zinc oxide film may differ due to the different deposition techniques (sputtering vs PVD) as well as the different applied thicknesses (50 vs 6 nm). A detailed surface study of the physicochemical/acid−base properties might give more insights into the observed differences in (de)protonation equilibrium.

3.3. In Situ Measurements in Aqueous Environment (D_2O). *3.3.1. ATR-FTIR and SFG Responses during Exposure to D_2O.* It has been demonstrated that for studying buried metal−paint interfaces the use of model metal substrates is a necessity to avoid experimental artifacts. The setups for in situ ATR-FTIR and SFG measurements during immersion of the zinc/zinc oxide−polyester system in D_2O are depicted in Figure 7. The inverse configuration for the SFG experiments has as an additional advantage that it can easily be combined with a liquid cell suitable for D_2O exposure measurements.

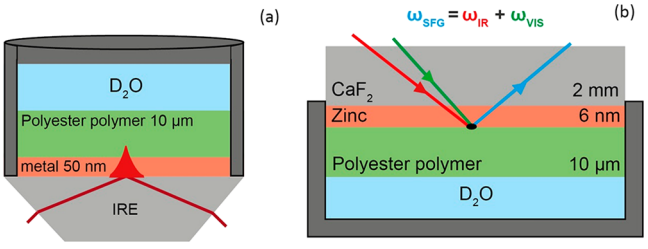

Figure 7. (a) ATR-FTIR and (b) SFG configuration for in situ measurements during immersion in D_2O.

In Figure 8 we present ATR-FTIR spectra in the frequency region 2000−4000 cm^{-1} at different time intervals after exposing the system to D_2O. The spectra illustrate an increasing O−D stretch band intensity (2473 cm^{-1}) with immersion time, indicative for D_2O uptake by the polyester coating. Meanwhile, C−H stretch vibrations at 2956, 2926, and 2859 cm^{-1} immediately appear as negative peaks. Because the in situ ATR-FTIR spectra are relative to the dry state, their negative intensity represents the replacement of CH_2 and CH_3 groups in the polyester interphase due to polymer swelling and D_2O accumulation at the interphase during submersion in D_2O. Furthermore, the O−H stretch vibration band at 3394

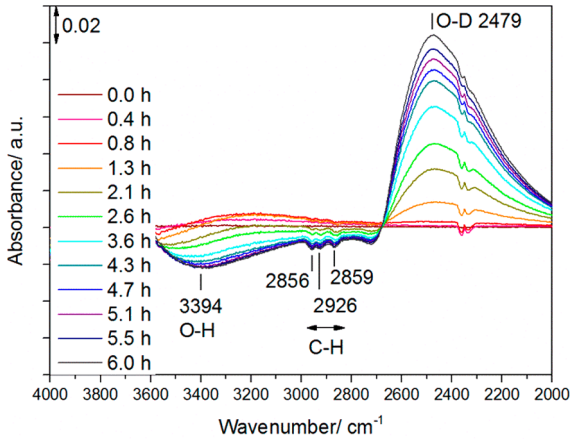

Figure 8. In situ ATR-FTIR spectra of polyester-coated zinc substrates during immersion in D_2O.

cm^{-1} also rapidly turns negative, illustrating interphase equilibrium reactions where hydrogen atoms are being exchanged by deuterium.

Figure 9a illustrates the carbonyl and carboxylate regions of the in situ ATR-FTIR spectra obtained during initial immersion of the zinc/zinc oxide−polyester system in D_2O. The illustrated spectra are relative to the dry state, given in Figure 3. It is noted that the ester carbonyl peak, positioned at 1729 cm^{-1}, has a negative peak area intensity, which further declines during prolonged immersion. On the other hand, asymmetric and symmetric carboxylate peaks, positioned at 1638 and 1471 cm^{-1}, respectively, appear positive and thus refer to an increased carboxylate fraction relative to the dry state. Because of this, it is inferred that ester groups are being hydrolyzed due to the migration of D_2O through the polyester coating. The hydrolysis of ester groups results in the formation of carboxylic acids, as indicated by the initial increase of the carbonyl peak at 1710 cm^{-1} during early immersion times. However, prolonged immersion times also turn the acid carbonyl peak negative, which can be attributed to their deprotonation forming carboxylate anions. As a result, the peak area intensity assigned to asymmetric carboxylate stretch vibrations increases with immersion time, attributed to the increased fraction of zinc−carboxylate complexes. However, after 1.1 h, a maximum carboxylate peak area has been reached, whereafter the peak area intensity declines again. It is thus shown that the formation of zinc−carboxylate complexes at the zinc oxide−polyester interphase occurs fast (i.e., within 1.1 h) but reduces equally as fast upon prolonged submersion in D_2O. Therefore, it is expected that the zinc−carboxylate complexes are highly susceptible to bond degradation in aqueous media, which can be attributed to their ionic character. To quantify the altered bonding density, the maximum peak areas shown in Figure 9a can be compared to those shown in Figure 3 representing the dry state. For the carboxyl peak a negative peak intensity of 0.006 au and a positive asymmetric carboxylate peak intensity of 0.003 au have been observed after 2.5 and 1.1 h of immersion, respectively. On the other hand, in the dry state, as shown in Figure 3, the carbonyl (C═O) and asymmetric carboxylate (COO^-_{as}) peak intensity is equal to 0.08 au. Expressed in percentage relative to the dry state, this corresponds to a reduction of interphase C═O bonds of 7.5% after 2.5 h and a maximum increase of 3.8% carboxylate bonds after 1.1 h of immersion.

https://dx.doi.org/10.1021/acs.jpcc.9b10775
J. Phys. Chem. C 2020, 124, 7127−7138

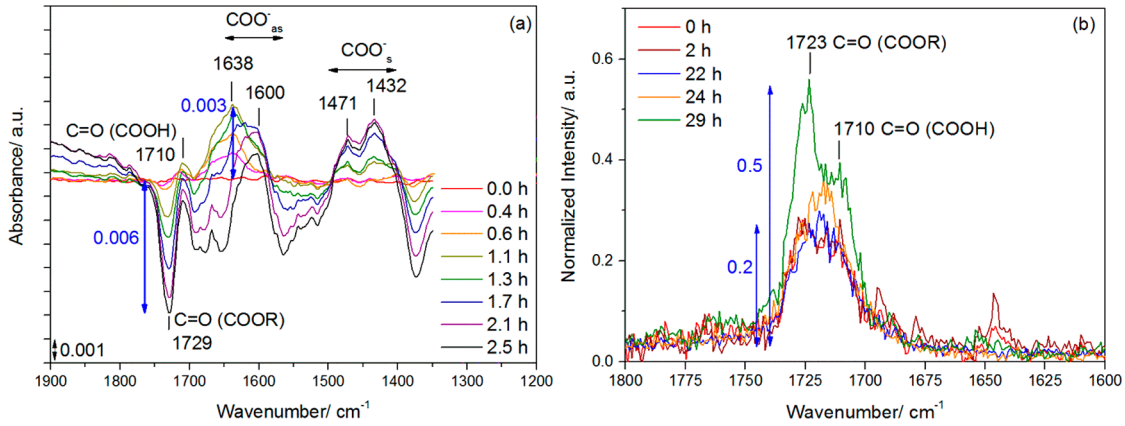

Figure 9. Evolution of polyester-coated zinc during exposure to D_2O obtained by (a) ATR-FTIR measurements, collected by using polyester-coated zinc prior to immersion as background; (b) SFG measurements.

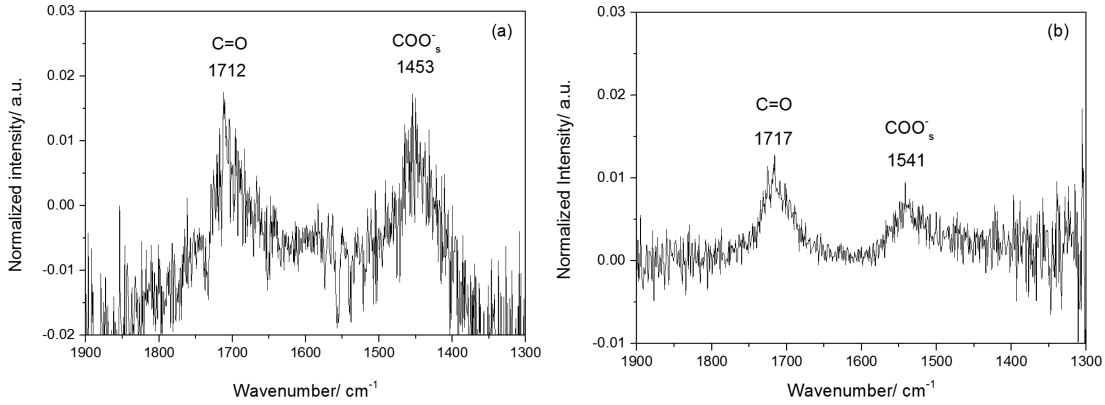

Figure 10. SFG spectra of the (a) CaF_2 and (b) zinc−polyester interface after 3 weeks submersion in D_2O.

In Figure 9b, the SFG response is shown at different delay times after exposure to D_2O. Similar to the measurements under dry conditions, deprotonated acid species at the zinc/zinc oxide surface are not being formed within 30 h of exposure to D_2O. Nonetheless, a significant increase in carbonyl SFG peak intensity (from 0.075 to 0.2 au) is noted. This increase is observed for both the major peak at 1723 cm^{-1} representative of ester groups as well as its shoulder at 1710 cm^{-1} representative of acid groups and can be attributed to a higher density of these groups near the zinc/zinc oxide surface and/or an increase in orientation upon exposure to D_2O. It is conceivable that the presence of D_2O increases the mobility of the polyester carbonyl and carboxylic acid groups leading to a better orientation toward zinc oxide and a higher SFG signal. This explanation would also explain the lag time of ∼22 h which is observed in the rise of the SFG signal; the SFG signal only starts to rise after a sufficient amount of D_2O has diffused through the polyester layer and has reached the interface with zinc/zinc oxide. Additional experiments using different polarization modes, such as PPP and SPS polarization combinations, might provide additional information in changes in orientation.

Figure 10a,b demonstrates SFG spectra obtained upon prolonged immersion times (>3 weeks) of the submersed two- and three-layered system, i.e., without and with zinc, respectively. It can be seen that the carbonyl (C═O) peak position shifts toward lower wavenumbers, i.e., 1712 and 1717 cm^{-1}, compared to those obtained in the dry state, illustrated in Figure 6d. The carbonyl shift indicates the hydrolytic degradation of ester groups forming carboxylic acids. Yet, more striking is the appearance of a second peak at 1453 and 1541 cm^{-1} at the polyester−CaF_2 and polyester−zinc oxide interface, respectively. Because asymmetric carboxylate stretch vibrations are expected to be far less SFG active in SSP polarization mode, this additional peak must be assigned to symmetric carboxylate (COO^-_s) stretch vibrations.[72,73] The eventual deprotonation of acid groups implies that prolonged immersion times cause a near-surface pH increase, yet this is shown to be a very slow process. The considerable difference in symmetric carboxylate peak position shown in Figure 10a,b indicates that different metal cations are involved in the formed metal−carboxylate complexes and thus evidence that a zinc layer still exists upon prolonged immersion. Although it is known that the IR frequency of carboxylate stretch vibrations depends on the interacting cation,[38] it is noted that the observed wavenumber for zinc−carboxylate bonds are rather high for symmetric carboxylate stretch vibrations. This high IR frequency can be associated with loosely bounded ionic zinc−carboxylate bonds, whereas the lower IR frequency, shown in Figure 10a, suggests that carboxylate anions are more strongly coordinated on calcium cations.[44]

3.3.3. Strengths, Limitations, and Further Perspectives. At this moment two different bonding mechanisms have been elucidated by using ATR-FTIR and SFG. Whereas the ATR-FTIR was shown to lead to deprotonation of carboxylic acid groups forming carboxylate species, SFG demonstrated much more stable acid groups, which remained protonated at the zinc oxide surface. It can be expected that different zinc oxide

https://dx.doi.org/10.1021/acs.jpcc.9b10775
J. Phys. Chem. C 2020, 124, 7127−7138

Table 3. Comparison of the Properties Specific to Spectroscopic Techniques ATR-FTIR and Broadband SFG

properties	ATR-FTIR	SFG
IR frequency region	4000−650 cm^{-1}	5000−1000 cm^{-1}
IR frequency range/ measurement	3350 cm^{-1}	±600 cm^{-1} (tunable)
selection rules	dipole of molecule must change during vibration	molecular vibrations have to be both IR- and Raman-active
	change of dipole must be the same as the direction of the electric field	the change of dipole must be the same as the direction of the electric field
		SF is selectively generated at surfaces and interfaces where symmetry is broken
		highly ordered/oriented molecular bonds are SF-active
probing depth	interphase (100−800 nm)	interface (one to several monolayers depending on the order in the noncentrosymmetric environment)
dynamic measurements (in situ)	relative to background	direct
light source intensity	low: nondestructive	high: can induce thermal effects
user-friendliness	very high	more hands-on

acid−base properties, resulting from the different application process, might shift the equilibrium toward more or less protonation. However, it is highly unlikely that the chemical nature of the zinc layer formed on the SFG samples is that different that it does not introduce any deprotonation reaction. This because isoelectric point values of zinc are in general situated around 9−10. Consequently, the interfacial sensitivity of the vibrational tools is considered to be majorly responsible for the probed differences in interfacial molecular information.

Nevertheless, further research is strongly recommended to optimize the metal deposition process in such a way that similar films can be applied for ATR-FTIR and SFG measurements. In this way, ATR-FTIR and SFG can be used as highly complementary tools. Furthermore, XPS analysis of the metallic zinc films prior to paint application is recommended to correlate observed bonding properties to the oxide's acid−base nature.[23]

Table 3 gives an overview of characteristics specific to ATR-FTIR and SFG. Obvious advantages of ATR-FTIR over SFG are its broad IR frequency region that can be covered during one single measurement. Conversely, using SFG, we have to define a smaller IR frequency region, with 1200 cm^{-1} being the lower wavenumber limit due to laser limitations. As a consequence, spectral features separated by more than 600 cm^{-1} cannot be followed simultaneously during in situ measurements. On the other hand, advantages of SFG over ATR-FTIR are its monolayer sensitivity and its selectivity for highly ordered/oriented structures as a result of the more strict selection rules of SFG. One of these additional selection rules of SFG compared to ATR-FTIR is the required ordering at the interface inducing symmetry breakage. Because of this requirement, information about orientation can be derived from SFG, which cannot be obtained by using ATR-FTIR. This can be even further extended using different polarization combinations, indicating tilt angles of molecular bonds at the interface. At the expense of these extended selection rules, other spectral information must be obtained by using ATR-FTIR. For example, since C−N═C stretch vibrations appear to be SFG inactive, interactions with the melamine-based cross-linker cannot be followed by using SFG, although this has been reported to contribute to interfacial bonding.[67] Yet, the information-rich ATR-FTIR spectrum has pros and cons; the high share of vibrational peaks can make the ATR-FTIR very complex and hard to interpret, whereas SFG spectra are generally more straightforward. As an example, spectral interference of asymmetric carboxylate vibrations by aromatic ring vibrations as well as OH-bending vibrations is not an issue for SFG measurements. Consequently, SFG allows to follow the dynamic behavior of carboxylate peaks in H_2O, whereas in situ ATR-FTIR stability studies on carboxylate bonds have to be performed in D_2O. The lack of interference by the O−H bending mode of water in SFG measurements comes with the advantage of controlling the pH of the aqueous solution more easily. Adding chemicals such as NaOH to increase pH or borate salts to buffer the interface pH introduces H_2O to the solution which might be undesired for in situ ATR-FTIR measurements. The possibility to use a wide variety of aqueous solutions infers that SFG can provide additional insights into the fundamentals of water and ionic mobility and interfacial bonding properties of metal oxide−polymer hybrid systems. This provides the opportunity to optimize and create new enhanced metallic/organic coating systems that are better resistant to degradation and can lead to an improved lifetime.

4. CONCLUSIONS

This work elucidated molecular organizations at zinc/zinc oxide polyester coating interfaces using two spectroscopic techniques: attenuated total reflection−Fourier transform infrared spectroscopy (ATR-FTIR) and sum frequency generation (SFG). It was shown that ATR-FTIR is an interphase (3D)-sensitive technique with probing depths of 250−400 nm in the frequency region of the carbonyl and carboxylate stretch vibrations, i.e., 2000−1200 cm^{-1}. SFG, on the other hand, is an interface (2D)-sensitive technique. ATR-FTIR illustrated the formation of carboxylate bonds when zinc oxide was present at the interphase region of the polyester coating. SFG measurements showed that at the interface with zinc/zinc oxide the carboxylic acid groups are stable and are not converted to carboxylate groups. Exposure of the polymer−zinc/zinc oxide system to D_2O leads to an increase of 3.5% of carboxylate bonds with respect to the dry state in the polymer phase. This conversion occurs within a few hours. SFG measurements show that the carbonyl and carboxylic acid groups near the interface with zinc/zinc oxide are much more stable and only after days start to be converted to carboxylate groups.

Additional recommendations on experimental design as well as future research perspectives have been proposed. Further developments in the use of ATR-FTIR and SFG as complementary techniques provide the opportunity to gain more insights into the fundamentals of water and ionic

https://dx.doi.org/10.1021/acs.jpcc.9b10775
J. Phys. Chem. C 2020, 124, 7127−7138

mobility and interfacial bonding properties metal oxide−polymer hybrid systems.

AUTHOR INFORMATION

Corresponding Author

Johannes M. C. Mol − *Department of Materials Science and Engineering, Research Group Corrosion Technology and Electrochemistry, Delft University of Technology, 2628 CD Delft, The Netherlands;* orcid.org/0000-0003-1810-5145; Email: J.M.C.Mol@tudelft.nl

Authors

Laura-Lynn I. Fockaert − *Netherlands Organization for Scientific Research (NWO), 3502 GA Utrecht, The Netherlands; Department of Materials Science and Engineering, Research Group Corrosion Technology and Electrochemistry, Delft University of Technology, 2628 CD Delft, The Netherlands*

Deborah Ganzinga-Jurg − *Research and Development, Surface Engineering-Coating Development, Tata Steel IJmuiden B.V., 1970 CA IJmuiden, The Netherlands*

Jan Versluis − *Research Group Ultrafast Spectroscopy, AMOLF, 1098 XG Amsterdam, The Netherlands*

Berend Boelen − *Research and Development, Surface Engineering-Coating Development, Tata Steel IJmuiden B.V., 1970 CA IJmuiden, The Netherlands*

Huib J. Bakker − *Research Group Ultrafast Spectroscopy, AMOLF, 1098 XG Amsterdam, The Netherlands;* orcid.org/0000-0003-1564-5314

Herman Terryn − *Department of Materials and Chemistry, Research Group Electrochemical Surface Engineering, Vrije Universiteit Brussel, 1050 Brussels, Belgium;* orcid.org/0000-0003-2639-5496

Complete contact information is available at: https://pubs.acs.org/10.1021/acs.jpcc.9b10775

Notes

The authors declare no competing financial interest.

ACKNOWLEDGMENTS

This research was performed under Project F81.3.13509 in the framework of the Partnership Program of the Materials Innovation Institute M2i and the Foundation for Fundamental Research on Matter (FOM), which is part of The Netherlands Organisation for Scientific Research NWO. The authors acknowledge Gavin Scott from AkzoNobel for the primer formulation and Kees Kwakernaak from TUDelft for sputtering the zinc films.

REFERENCES

(1) Buchheit, R. G. *Handbook of Environmental Degradation of Materials; Corrosion Resistant Coatings and Paints*; Kutz, M., Ed.; William Andrew, Elsevier: 2005.

(2) Pocius, A. *Adhesion and Adhesives Technology*, 3rd ed.; Carl Hanser Verlag: 2012.

(3) Comyn, J. *Adhesion Science; Contact Angles in the Study of Adhesion*; The Royal Society of Chemistry: 1997.

(4) Kinloch, A. J. *Adhesion and Adhesives*; 1st ed.; Chapman and Hall: 1987.

(5) González-Orive, A.; Giner, I.; de los Arcos, T.; Keller, A.; Grundmeier, G. Analysis of Polymer/Oxide Interfaces under Ambient Conditions − An Experimental Perspective. *Appl. Surf. Sci.* **2018**, *442*, 581−594.

(6) Hinder, S. J.; Lowe, C.; Maxted, J. T.; Watts, J. F. The Morphology and Topography of Polymer Surfaces and Interfaces Exposed by Ultra-Low-Angle Microtomy. *J. Mater. Sci.* **2005**, *40* (2), 285−293.

(7) Ghaffari, M.; Saeb, M. R.; Ramezanzadeh, B.; Taheri, P. Demonstration of Epoxy/Carbon Steel Interfacial Delamination Behavior: Electrochemical Impedance and X-Ray Spectroscopic Analyses. *Corros. Sci.* **2016**, *102*, 326−337.

(8) Leadley, S. R.; Watts, J. F. The Use of Monochromated XPS to Evaluate Acid- Base Interactions at the PMMA/Oxidised Metal Interface. *J. Adhes.* **1997**, *60*, 175−196.

(9) Watts, J. F.; Castle, J. E. Determination of Adsorption Isotherms by XPS and ToF-SIMS: Their Role in Adhesion Science. *Int. J. Adhes. Adhes.* **1999**, *19* (6), 435−443.

(10) Pletincx, S.; Trotochaud, L.; Fockaert, L.-L.; Mol, J. M. C.; Head, A. R.; Karslıoğlu, O.; Bluhm, H.; Terryn, H.; Hauffman, T. In Situ Characterization of the Initial Effect of Water on Molecular Interactions at the Interface of Organic/Inorganic Hybrid Systems. *Sci. Rep.* **2017**, *7*, 45123.

(11) Pletincx, S.; Marcoen, K.; Trotochaud, L.; Fockaert, L.-L.; Mol, J. M. C.; Head, A. R.; Karslioğlu, O.; Bluhm, H.; Terryn, H.; Hauffman, T. Unravelling the Chemical Influence of Water on the PMMA/Aluminum Oxide Hybrid Interface In Situ. *Sci. Rep.* **2017**, *7* (1), 13341.

(12) Taheri, P.; Terryn, H.; Mol, J. M. C. Studying Interfacial Bonding at Buried Polymer−Zinc Interfaces. *Prog. Org. Coat.* **2015**, *89*, 323−331.

(13) Sababi, M.; Terryn, H.; Mol, J. M. C. The Influence of a Zr-Based Conversion Treatment on Interfacial Bonding Strength and Stability of Epoxy Coated Carbon Steel. *Prog. Org. Coat.* **2017**, *105*, 29−36.

(14) Öhman, M.; Persson, D. ATR-FTIR Kretschmann Spectroscopy for Interfacial Studies of a Hidden Aluminum Surface Coated with a Silane Film and Epoxy I. Characterization by IRRAS and ATR-FTIR. *Surf. Interface Anal.* **2012**, *44* (2), 133−143.

(15) Öhman, M.; Persson, D.; Leygraf, C. In Situ ATR-FTIR Studies of the Aluminium/Polymer Interface upon Exposure to Water and Electrolyte. *Prog. Org. Coat.* **2006**, *57*, 78−88.

(16) Beentjes, P. C. J.; Van den Brand, J.; De Wit, J. H. W. Interaction of Ester and Acid Groups Containing Organic Compounds with Iron Oxide Surfaces. *J. Adhes. Sci. Technol.* **2006**, *20* (1), 1−18.

(17) van den Brand, J.; Blajiev, O.; Beentjes, P. C. J.; Terryn, H.; de Wit, J. H. W. Interaction of Anhydride and Carboxylic Acid Compounds with Aluminum Oxide Surfaces Studied Using Infrared Reflection Absorption Spectroscopy. *Langmuir* **2004**, *20* (15), 6308−6317.

(18) Dobson, K. D.; McQuillan, A. J. In Situ Infrared Spectroscopic Analysis of the Adsorption of Aromatic Carboxylic Acids to TiO_2, ZrO2, Al2O3, and Ta2O5 from Aqueous Solutions. *Spectrochim. Acta, Part A* **2000**, *56* (3), 557−565.

(19) Dobson, K. D.; McQuillan, A. J. An Infrared Spectroscopic Study of Carbonate Adsorption to Zirconium Dioxide Sol-Gel Films from Aqueous Solutions. *Langmuir* **1997**, *13* (13), 3392−3396.

(20) Dobson, K. D.; Mcquillan, A. J. In Situ Infrared Spectroscopic Analysis of the Adsorption of Aliphatic Carboxylic Acids to TiO_2, ZrO2, Al2O3, and Ta2O5 from Aqueous Solutions. *Spectrochim. Acta, Part A* **1999**, *55*, 1395−1405.

(21) Taheri, P.; Hauffman, T.; Mol, J. M. C.; Flores, J. R.; Hannour, F.; de Wit, J. H. W.; Terryn, H. Electrochemical Analysis of the Adsorption and Desorption Behaviors of Carboxylic Acid and Anhydride Monomers onto Zinc Surfaces. *Electrochim. Acta* **2011**, *56* (25), 9317−9323.

(22) Taheri, P.; Wielant, J.; Hauffman, T.; Flores, J. R.; Hannour, F.; de Wit, J. H. W.; Mol, J. M. C.; Terryn, H. A Comparison of the Interfacial Bonding Properties of Carboxylic Acid Functional Groups on Zinc and Iron Substrates. *Electrochim. Acta* **2011**, *56* (4), 1904−1911.

(23) Fockaert, L. I.; Pletincx, S.; Boelen, B.; Hauffman, T.; Terryn, H.; Mol, J. M. C. Effect of Zirconium-Based Conversion Treatments of Zinc, Aluminium and Magnesium on the Chemisorption of Ester-Functionalized Molecules. *Appl. Surf. Sci.* **2020**, *508*, 145199−145210.
(24) Fockaert, L. I.; Taheri, P.; Abrahami, S. T.; Boelen, B.; Terryn, H.; Mol, J. M. C. Zirconium-Based Conversion Film Formation on Zinc, Aluminium and Magnesium Oxides and Their Interactions with Functionalized Molecules. *Appl. Surf. Sci.* **2017**, *423*, 817−828.
(25) Roncaroli, F.; Blesa, M. A. Kinetics of Adsorption of Oxalic Acid on Different Titanium Dioxide Samples. *J. Colloid Interface Sci.* **2011**, *356* (1), 227−233.
(26) Kirwan, L. J.; Fawell, P. D.; Van Bronswijk, W. In Situ FTIR-ATR Examination of Poly(Acrylic Acid) Adsorbed onto Hematite at Low PH. *Langmuir* **2003**, *19* (14), 5802−5807.
(27) Wilson, P. T.; Briggman, K. A.; Wallace, W. E.; Stephenson, J. C.; Richter, L. J. Selective Study of Polymer/Dielectric Interfaces with Vibrationally Resonant Sum Frequency Generation via Thin-Film Interference. *Appl. Phys. Lett.* **2002**, *80* (17), 3084−3086.
(28) Briggman, K. A.; Stephenson, J. C.; Wallace, W. E.; Richter, L. J. Absolute Molecular Orientational Distribution of the Polystyrene Surface. *J. Phys. Chem. B* **2001**, *105* (14), 2785−2791.
(29) O'Brien, D. B.; Massari, A. M. Simulated Vibrational Sum Frequency Generation from a Multilayer Thin Film System with Two Active Interfaces. *J. Chem. Phys.* **2013**, *138* (15), 154708.
(30) Lu, Z.; Karakoti, A.; Velarde, L.; Wang, W.; Yang, P.; Thevuthasan, S.; Wang, H. F. Dissociative Binding of Carboxylic Acid Ligand on Nanoceria Surface in Aqueous Solution: A Joint in Situ Spectroscopic Characterization and First-Principles Study. *J. Phys. Chem. C* **2013**, *117* (46), 24329−24338.
(31) Adhikari, N. M.; Premadasa, U. I.; Cimatu, K. L. A. Sum Frequency Generation Vibrational Spectroscopy of Methacrylate-Based Functional Monomers at the Hydrophilic Solid-Liquid Interface. *Phys. Chem. Chem. Phys.* **2017**, *19* (32), 21818−21828.
(32) Sthoer, A.; Hladílková, J.; Lund, M.; Tyrode, E. Molecular Insight into Carboxylic Acid-Alkali Metal Cations Interactions: Reversed Affinities and Ion-Pair Formation Revealed by Non-Linear Optics and Simulations. *Phys. Chem. Chem. Phys.* **2019**, *21* (21), 11329−11344.
(33) Boiziau, C.; Lecayon, G. Adhesion of Polymers to Metals : A Review of the Results Obtained Studying a Model System. *Surf. Interface Anal.* **1988**, *12*, 475−485.
(34) Marsh, J.; Minel, L.; Barthes-Labrousse, M. G.; Gorse, D. Interaction of Epoxy Model Molecules with Aluminium, Anodised Titanium and Copper Surfaces: An XPS Study. *Appl. Surf. Sci.* **1998**, *133* (4), 270−286.
(35) Wielant, J.; Hauffman, T.; Blajiev, O.; Hausbrand, R.; Terryn, H. Influence of the Iron Oxide Acid-Base Properties on the Chemisorption of Model Epoxy Compounds Studied by XPS. *J. Phys. Chem. C* **2007**, *111* (35), 13177−13184.
(36) Taheri, P.; Lill, K.; De Wit, J. H. W.; Mol, J. M. C.; Terryn, H. Effects of Zinc Surface Acid-Based Properties on Formation Mechanisms and Interfacial Bonding Properties of Zirconium-Based Conversion Layers. *J. Phys. Chem. C* **2012**, *116* (15), 8426−8436.
(37) Deacon, G. B.; Huber, F.; Phillips, R. J. Diagnosis of the Nature of Carboxylate Coordination from the Direction of Shifts of Carbon-Oxygen Stretching Frequencies. *Inorg. Chim. Acta* **1985**, *104*, 41−45.
(38) Tackett, J. E. FT-IR Characterization of Metal Acetates in Aqueous Solution. *Appl. Spectrosc.* **1989**, *43* (3), 483−489.
(39) Tannenbaum, R.; King, S.; Lecy, J.; Tirrell, M.; Potts, L. Infrared Study of the Kinetics and Mechanism of Adsorption of Acrylic Polymers on Alumina Surfaces. *Langmuir* **2004**, *20* (11), 4507−4514.
(40) Taheri, P.; Terryn, H.; Mol, J. M. C. An in Situ Study of Amine and Amide Molecular Interaction on Fe Surfaces. *Appl. Surf. Sci.* **2015**, *354*, 242−249.
(41) Lu, X.; Shephard, N.; Han, J.; Xue, G.; Chen, Z. Probing Molecular Structures of Polymer/Metal Interfaces by Sum Frequency Generation Vibrational Spectroscopy. *Macromolecules* **2008**, *41*, 8770−8777.
(42) Zhang, C.; Hankett, J.; Chen, Z. *Molecular Level Understanding of Adhesion Mechanisms at the Epoxy/Polymer Interfaces*, 2012.
(43) Tang, C. Y.; Allen, H. C. Ionic Binding of Na + versus K + to the Carboxylic Acid Headgroup of Palmitic Acid Monolayers Studied by Vibrational Sum Frequency Generation Spectroscopy. *J. Phys. Chem. A* **2009**, *113* (26), 7383−7393.
(44) Tang, C. Y.; Huang, Z.; Allen, H. C. Binding of Mg2+ and Ca2+ to Palmitic Acid and Deprotonation of the Cooh Headgroup Studied by Vibrational Sum Frequency Generation Spectroscopy. *J. Phys. Chem. B* **2010**, *114* (51), 17068−17076.
(45) Abel, M.; Watts, J. F.; Digby, R. P.; Watts, J. F.; Digby, R. P.; Influence, T. H. E.; Abel, M.; Watts, J. F.; Digby, R. P. The Influence of Process Parameters on the Interfacial Chemistry of γ -GPS on Aluminium: A Review. *J. Adhes.* **2004**, *80*, 291−312.
(46) Abbott, S. *Adhesion Science: Principles and Practice*; DEStech Publications, Inc.: 2015.
(47) Papaj, E. A.; Mills, D. J.; Jamali, S. S. Effect of Hardener Variation on Protective Properties of Polyurethane Coating. *Prog. Org. Coat.* **2014**, *77* (12), 2086−2090.
(48) Taheri, P.; Flores, J. R.; Hannour, F.; De Wit, J. H. W.; Terryn, H.; Mol, J. M. C. In Situ Study of Buried Interfacial Bonding Mechanisms of Carboxylic Polymers on Zn Surfaces. *J. Phys. Chem. C* **2013**, *117* (7), 3374−3382.
(49) Mangolini, F.; Rossi, A. *Attenuated Total Reflection-Fourier Transform Infrared Spetroscopy: A Powerful Tool for Investigating Polymer Surfaces and Interfaces*; Walter de Gruyter: 2014.
(50) Osawa, M. *Near-Field Optics and Surface Plasmon Polaritons; Surface-Enhanced Infrared Absorption*, 1st ed.; Kawata, S., Ed.; Springer-Verlag: Berlin, 2001; Vol. *81*.
(51) Osawa, M.; Ataka, K.; Yoshii, K.; Nishikawa, Y. Surface-Enhanced Infrared Spectroscopy: The Origin of the Absorption Enhancement and Band Selection Rule in the Infrared Spectra of Molecules Adsorbed on Fine Metal Particles. *Appl. Spectrosc.* **1993**, *47* (9), 1497−1502.
(52) Harrick, N. J. Study of Physics and Chemistry of Surfaces from Frustrated Total Internal Reflections. *Phys. Rev. Lett.* **1960**, *4* (5), 224−226.
(53) Ishida, K. P.; Griffiths, P. R. Theoretical and Experimental Investigation of Internal Reflection at Thin Copper Films Exposed to Aqueous Solutions. *Anal. Chem.* **1994**, *66* (4), 522−530.
(54) Taheri, P.; De Wit, J. H. W.; Terryn, H.; Mol, J. M. C. In Situ Study of Buried Metal-Polymer Interfaces Exposed to an Aqueous Solution by an Integrated ATR-FTIR and Electrochemical Impedance Spectroscopy System. *J. Phys. Chem. C* **2013**, *117* (40), 20826−20832.
(55) Lu, X.; Xue, G.; Wang, X.; Han, J.; Han, X.; Hankett, J.; Li, D.; Chen, Z. Directly Probing Molecular Ordering at the Buried Polymer/Metal Interface 2: Using P-Polarized Input Beams. *Macromolecules* **2012**, *45* (15), 6087−6094.
(56) Sun, S.; Tian, C.; Shen, Y. R. Surface Sum-Frequency Vibrational Spectroscopy of Nonpolar Media. *Proc. Natl. Acad. Sci. U. S. A.* **2015**, *112* (19), 5883−5887.
(57) Myers, J. N.; Chen, Z. Polymer Molecular Behaviors at Buried Polymer/Metal and Polymer/Polymer Interfaces and Their Relations to Adhesion in Packaging. *J. Adhes.* **2017**, *93* (13), 1081−1103.
(58) Lu, X.; Shephard, N.; Han, J.; Xue, G.; Chen, Z. Probing Molecular Structures of Polymer/Metal Interfaces by Sum Frequency Generation Vibrational Spectroscopy. *Macromolecules* **2008**, *41*, 8770−8777.
(59) Israelachvili, J.; Min, Y.; Akbulut, M.; Alig, A.; Carver, G.; Greene, W.; Kristiansen, K.; Meyer, E.; Pesika, N.; Rosenberg, K.; et al. Recent Advances in the Surface Forces Apparatus (SFA) Technique. *Rep. Prog. Phys.* **2010**, *73* (3), 036601.
(60) Myers, J. N.; Chen, Z. Polymer Molecular Behaviors at Buried Polymer/Metal and Polymer/Polymer Interfaces and Their Relations to Adhesion in Packaging. *J. Adhes.* **2017**, *93*, 1081−1103.
(61) Johnson, C. M.; Tyrode, E.; Baldelli, S.; Rutland, M. W.; Leygraf, C. A Vibrational Sum Frequency Spectroscopy Study of the Liquid - Gas Interface of Acetic Acid - Water Mixtures : 1. Surface Speciation. *J. Phys. Chem. B* **2005**, *109*, 321−328.

https://dx.doi.org/10.1021/acs.jpcc.9b10775
J. Phys. Chem. C 2020, 124, 7127−7138

(62) Myers, J. N.; Chen, Z. Surface Plasma Treatment Effects on the Molecular Structure at Polyimide/Air and Buried Polyimide/Epoxy Interfaces. *Chin. Chem. Lett.* **2015**, *26*, 449−454.
(63) Richter, L. J.; Petralli-Mallow, T. P.; Stephenson, J. C. Vibrationally Resolved Sum-Frequency Generation with Broad-Bandwidth Infrared Pulses. *Opt. Lett.* **1998**, *23* (20), 1594.
(64) Maier, S. A. *Plasmonics: Fundamentals and Applications*; Springer Science & Business Media: 2007.
(65) Querry, M. R. *Optical Constants of Minerals and Other Materials from the Millimeter to the Ultraviolet, Contractor Report CRDEC-CR-88009*, 1987.
(66) Barnes, W. L.; Dereux, A.; Ebbesen, T. W. Surface Plasmon Subwavelength Optics. *Nature* **2003**, *424* (6950), 824−830.
(67) Fockaert, L. I.; Pletincx, S.; Ganzinga-Jurg, D.; Boelen, B.; Hauffman, T.; Terryn, H.; Mol, J. M. C. Chemisorption of Polyester Coatings on Zirconium-Based Conversion Coated Multi-Metal Substrates and Their Stability in Aqueous Environment. *Appl. Surf. Sci.* **2020**, *508*, 144771−144781.
(68) Lu, X.; Zhang, C.; Ulrich, N.; Xiao, M.; Ma, Y. H.; Chen, Z. Studying Polymer Surfaces and Interfaces with Sum Frequency Generation Vibrational Spectroscopy. *Anal. Chem.* **2017**, *89* (1), 466−489.
(69) Lu, X.; Li, B.; Zhu, P.; Xue, G.; Li, D. Illustrating Consistency of Different Experimental Approaches to Probe the Buried Polymer/Metal Interface Using Sum Frequency Generation Vibrational Spectroscopy. *Soft Matter* **2014**, *10* (29), 5390−5397.
(70) George, S. *Infrared and Raman Characteristic Group Frequencies*, 3rd ed.; John Wiley & Sons, Inc.: 2001.
(71) Coates, J. *Encyclopedia of Analytical Chemistry, Interpretation of Infrared Spectra, A Practical Approach*; Meyers, R. A., Ed.; John Wiley & Sons, Ltd.
(72) Gan, W.; Wu, D.; Zhang, Z.; Feng, R. R.; Wang, H. F. Polarization and Experimental Configuration Analyses of Sum Frequency Generation Vibrational Spectra, Structure, and Orientational Motion of the Air/Water Interface. *J. Chem. Phys.* **2006**, *124* (11), 114705.
(73) Tyrode, E.; Hedberg, J. A Comparative Study of the CD and CH Stretching Spectral Regions of Typical Surfactants Systems Using VSFS: Orientation Analysis of the Terminal CH 3 and CD 3 Groups. *J. Phys. Chem. C* **2012**, *116* (1), 1080−1091.

https://dx.doi.org/10.1021/acs.jpcc.9b10775
J. Phys. Chem. C 2020, 124, 7127−7138